NASA TECHNICAL NOTE

NASA TN D-2859

LOW-SPEED WIND-TUNNEL TESTS OF A LARGE-SCALE INFLATABLE STRUCTURE PARAGLIDER

by Berl Gamse, Kenneth W. Mort, and Paul F. Yaggy

Ames Research Center

Moffett Field, Calif.

NATIONAL AERONAUTICS AND SPACE ADMINISTRATION • WASHINGTON, D. C. • JUNE 1965

NASA TN D-2859

LOW-SPEED WIND-TUNNEL TESTS OF A LARGE-SCALE INFLATABLE STRUCTURE PARAGLIDER

By Berl Gamse, Kenneth W. Mort, and Paul F. Yaggy

Ames Research Center
Moffett Field, Calif.

NATIONAL AERONAUTICS AND SPACE ADMINISTRATION

For sale by the Clearinghouse for Federal Scientific and Technical Information
Springfield, Virginia 22151 – Price $2.00

LOW-SPEED WIND-TUNNEL TESTS OF A LARGE-SCALE INFLATABLE STRUCTURE PARAGLIDER

By Berl Gamse, Kenneth W. Mort,
and Paul F. Yaggy
Ames Research Center

SUMMARY

25596

The paraglider tested was a full-scale model from a specific program to develop a recovery system for capsule-type spacecraft. It was designed and constructed so that it would be suitable for flight testing after the wind-tunnel tests. It had a leading-edge sweep angle of 55°, a sail flat pattern sweep angle of 52.5°, and a keel length of 30 feet.

The results of tests reported herein are concerned with the performance and longitudinal aerodynamic characteristics of the paraglider. The maximum lift-to-drag ratio obtained was about 4.0. The minimum angle of attack which could be obtained was limited by severe oscillations of the wing. Maximum loading conditions were limited sometimes by similar oscillations.

Aeroelastic deformations of the wing and suspension system caused significant changes in the aerodynamic characteristics. The maximum load which could be sustained without buckling varied under repeated loadings. These aeroelastic characteristics would be difficult to predict because of the inelastic load-deformation properties of the materials from which the structure is made.

Authors

INTRODUCTION

A considerable number of investigations of paragliders have been made at small scale, some of which have been reported in references 1 through 3. Among the many applications which have been proposed is a paraglider with an inflatable frame structure to be used for the recovery of manned, capsule-type spacecraft. Such a system could increase the glide range beyond that obtained with present recovery systems while retaining such factors as lightweight, compactness of storage, and deployment reliability. The spacecraft would be suspended below the paraglider and would be maneuvered by shifting the center of gravity of the system relative to the center of pressure. When deflated, the wing could be packed and deployed in a manner similar to that used for parachutes.

The investigation reported herein was conducted in the Ames 40- by 80-Foot Wind Tunnel and was part of a specific program to develop an inflatable frame paraglider system for flight tests.

NOTATION

C_D	drag coefficient, $\frac{D}{qS}$
C_L	lift coefficient, $\frac{L}{qS}$
C_m	pitching-moment coefficient, $\frac{\text{pitching moment}}{qSl_k}$
D	drag force, lb
L	lift force, lb
l	suspension line length measured from capsule attachment to the load distributor curtain attachment
l_k	keel length, reference, ft
q	dynamic pressure, psf
S	deployed wing area, nominal, reference, ft^2
T_o	preset tension in keel cambering cable, lb
X_{cp}	location of center of pressure on keel center line, percent of keel length
α_c	angle of attack of simulated capsule, deg
α_k	angle of attack of wing keel, deg (see Instrumentation and Data Reduction section)
Δ_{p_i}	differential internal pressure of wing structure, psi
θ	camber angle (see fig. 9(a)), deg

Subscripts

a	aft keel line
b	moment reference center at assumed capsule center of gravity
c	leading-edge boom line
d	diagonal keel line

f forward keel line

w moment reference center at wing center of gravity

The forces and moments are presented with respect to a wind axes system with moment reference centers as shown in figure 2(a).

MODEL DESCRIPTION

The paraglider model, designed and constructed by North American Aviation (figs. 1 and 2), consisted of four main parts: (1) the inflatable structure, (2) the sails or membranes, (3) the load distribution system, and (4) the suspension cables. The design of the wing made it suitable for flight testing. Figures 1 and 2 and table I present the pertinent information on the dimensions and materials used in the construction of the model.

The inflatable structure of the wing (fig. 2(b)) was composed of a keel boom and two leading-edge booms joined at their forward ends to form an apex; spreader bars located between each leading-edge boom and the keel boom maintained a leading-edge sweep angle of 55° under load. The structure was pressurized through a hose which passed up the forward suspension line and connected to the wing at the apex (see fig. 1). The differential internal pressure was held at 15.7 psi except during particular tests noted.

The fabric sails spanning the areas between the leading-edge and keel booms, when laid out in a flat pattern, had a sweep angle of 52.5°. Each sail met the inflatable structure at single lines of contact along the forward element of the leading-edge booms and the upper element of the keel boom. A nylon boltrope passed through the trailing edge of each sail and was attached to the ends of each boom. The boltrope provided tension in the trailing edge of the sail, thereby reducing sail flutter. The boltrope was 4 percent shorter than the flat pattern length of the sail trailing edge.

The wing load distribution system consisted of fabric "curtains" which went around the booms and attached to the sail. A nylon cable passed through the lower edge of the curtains and the cable ends attached to the ends of the booms. The lower edge of the curtains had scalloped, parabolic shapes. The suspension lines were attached to the curtains as shown in figure 2(a).

Each of the five suspension lines consisted of a length of a steel cable connected to a short length of nylon cable attached to the load distributor. The nylon segment was provided to facilitate packing the wing and to absorb the shock during deployment. The length of the forward keel suspension line varied from 0.61 l_k to 0.67 l_k. The sum of the leading-edge suspension line lengths was constant at 1.24 l_k with the lengths of the lines varied differentially to correct the wing roll attitude. The aft and diagonal suspension line lengths were varied differentially such that $l_a + l_d = 1.02\ l_k$.

The suspension lines were attached to a platform which could be pitched from $\alpha_c = -13^\circ$ to $+21^\circ$ with the attachment points located as they would be on a capsule type spacecraft (fig. 2(a)). This platform will henceforth be referred to as the simulated capsule or capsule.

Two devices were added to the inflatable structure in an attempt to control and/or decrease the aeroelastic distortion of the wing which was noted during the test. These devices were sleeves on the spreader bars and a "bowstring" device on the keel boom. Two sets of spreader bar sleeves were tested: One set was made from coated Dacron fabric of the same order of thickness as the spreader bar wall to retain the compact storage feature; the other set was made from 0.025-inch-thick aluminum and made the spreader bars essentially rigid. The bowstring device consisted of a Dacron strap (7000-lb test strength) connected to fabric harnesses at the leading and trailing edges of the keel. It passed through an "eye" fitting at the diagonal line attachment station through which it was free to slide fore and aft as required by variations in the tension. The tension could be preset to produce positive camber in the keel boom prior to testing. The preset tension was 1000 pounds unless otherwise noted.

INSTRUMENTATION AND DATA REDUCTION

The forces developed by the model were measured by the wind-tunnel six-component balance system. The keel angle of attack was the average angle and was determined by sighting three points along the keel with two transits. In this way the wing was also located in space so that the moment reference center on the wing relative to the capsule was directly determined. The shape of the keel was indicated by three pendulum potentiometers fixed at stations 0.09 l_k, 0.49 l_k, and 0.93 l_k on the keel. The tension in the keel-cambering cable was measured by a single axis load cell.

Forces and pitching moments were computed for a wind axis system with the moment reference center at the assumed capsule center of gravity unless otherwise noted, in which case it was at the wing moment reference center (see fig. 2(a)). Appropriate tare corrections were made for the wing weight (lift and pitching moment) and attachment platform aerodynamics (lift, drag, and pitching moment). Thus the data presented are those of a weightless wing and suspension system.

TESTING PROCEDURE

The longitudinal aerodynamic characteristics of the model were obtained by varying the capsule angle of attack with several combinations of suspension line lengths. Results were obtained with and without the two sets of spreader bar sleeves, and with the keel-cambering device at several preset tensions.

The effects of dynamic pressure (wing loading) were examined at constant capsule attitude for two internal boom pressures with and without the fabric

spreader bar stiffeners. The procedure was first to increase the dynamic pressure until a spreader bar buckled. The dynamic pressure was then reduced until the spreader bar unbuckled and the procedure was repeated to determine the effects of repeated loading.

RESULTS AND DISCUSSION

Basic Aerodynamic Characteristics

Figures 3 through 5 present the basic aerodynamic characteristics of the wing with and without the two spreader bar sleeves for several combinations of suspension line lengths. The maximum lift-to-drag ratio obtained was about 4.0 at a lift coefficient of about 1.1. The range of lift coefficients that could be tested was limited by oscillation of the wing relative to the simulated capsule attachments. The minimum lift coefficient (about 0.7 to 0.8) was determined by a severe roll-yaw coupled oscillation which was independent of suspension line configuration. Operation at higher lift coefficients was sometimes limited by a similar coupled roll-yaw oscillation of lower intensity accompanied by severe low amplitude pitch oscillations. The lift coefficient at which these oscillations occurred appeared to depend on suspension line configuration. Another test-range limitation was suspension line unloading. With certain line settings and with the simulated capsule at low angles of attack, the diagonal line would become slack, and with some of the other line settings and with the capsule at high angles of attack, the forward and/or rear lines would become slack. This unloading occurred when the force vector on the wing passed outside the capsule attachment points and has been observed during small-scale model tests of paragliders reported in reference 2.

It can be seen from the pitching-moment results of figures 3 through 5 that, for many of the line settings, the pitching moment is less stable at the two extremes of the capsule angle-of-attack range. A similar loss in stability was observed in reference 2 when one of the suspension lines became slack. However, for the present model the loss in stability occurred sometimes with and sometimes without slack suspension lines.

Aeroelastic Characteristics

The effects of aeroelasticity on this highly flexible system were evident in the test results. These were identified more specifically as wing frame and suspension system flexibility and were studied in more detail in terms of spreader bar buckling and keel-boom bending.

Wing frame and suspension system flexibility.- If the wing frame and the suspension system had been inelastic, it would be expected that all of the data, when referred to the wing angle of attack, would be identical. Figure 6 presents the lift and pitching-moment results of figure 3 referred to the wing angle of attack and wing moment reference center. From these results it can be seen that the aerodynamic characteristics vary significantly with line length, indicating that the shape of the wing frame varied considerably with

line configuration. It should also be noted from a comparison of figures 3 and 6 that $\partial C_L/\partial \alpha_k \neq \partial C_L/\partial \alpha_c$. Thus, the wing does not hold a constant incidence angle relative to the capsule because of the flexibility of the wing and suspension lines. Prediction of the wing attitude and position with respect to the capsule would require proper accounting for these aeroelastic effects. However, this accounting would be difficult because of the nonlinear and nonrepetitive load-deformation characteristics of the materials from which the structure is made.

Spreader bar deformation.- In figure 7 a direct comparison of the aerodynamic characteristics is made for a given line setting for the wing with and without the two spreader bar sleeves. This figure indicates that unless the spreader bars are buckled, the differences in the aerodynamic characteristics are small. It can be seen that when one of the spreader bars buckled there was a reduction of about 20 percent in lift and the maximum lift-to-drag ratio was reduced to about 3.7. However, the accompanying change in trim ($C_{m_b} = 0$) angle of attack was 3°.

In figure 8 the effects of varying dynamic pressure at a constant capsule angle of attack of -6° (i.e., the effects of wing loading) are shown for the configurations with no spreader bar stiffening and with the fabric stiffener. It is apparent that the spreader bar resistance to deformation or buckling was not only sensitive to internal pressure and wall thickness but to the number of cycles that it had been loaded. When the spreader bar buckled as the dynamic pressure was increased, there was little change in the variation of drag and pitching-moment coefficient with free-stream dynamic pressure even though the reduction in lift coefficient was as large as 20 percent. When the spreader bar buckled, the wing rolled to one side. This was corrected by differentially lengthening and shortening the leading-edge suspension lines. However, nearly all of the available lateral control was required.

The data in figure 8 also show that as the wing is more highly loaded the center of pressure moves forward (moment becoming more positive). This was due not only to spreader bar deformation but also to deformation of the keel boom under load.

Keel-boom deformation.- Figure 9(a) shows the effect of lift coefficient on keel camber angle for three preset bowstring tensions. It is apparent that as lift coefficient increases, the wing keel camber angle decreases at the same rate regardless of the preset bowstring tension. In addition this figure shows that the bowstring tension increases with lift coefficient. The last data point shown for 1000-lb preset tension indicates that the keel boom had deformed inelastically.

Figure 9(b) shows the effect on the aerodynamic characteristics of varying the preset bowstring tension or the initial keel camber. The effect of increasing this bowstring tension is an aft shift in the center of pressure, as evidenced by the decreasing pitching moment for the same lift coefficient and capsule angle of attack. At high lift coefficients the increased preloading results in slightly lower drag coefficients.

The effects of preloading the bowstring cable varied in that the keel shape was not always repeatable for a particular preload. As with the spreader bars the keel had a "memory" of past loadings. An extreme case was experienced when, for a configuration previously tested satisfactorily, the keel assumed a much more highly cambered shape than before and the wing could not be flown.

CONCLUDING REMARKS

The tests of a large-scale paraglider indicated that a maximum lift-to-drag ratio of about 4.0 could be obtained. A buckled spreader bar decreased this ratio to about 3.7 and appeared to cause little change in trim angle of attack, but resulted in a loss in lift and lateral asymmetry of loading on the wing. Correction of the resulting roll-off required nearly all available lateral control leaving none for maneuvering in flight.

The minimum keel angle of attack which could be tested was limited by severe oscillation of the wing relative to the body attachments. Maximum loading conditions were sometimes limited by similar oscillations. Aeroelastic deformations of the wing and suspension system caused significant changes in the aerodynamic characteristics which would be difficult to predict. The maximum load which could be sustained without buckling varied under repeated loadings. These factors probably would limit the flight envelope.

Ames Research Center
National Aeronautics and Space Administration
Moffett Field, Calif., Mar. 29, 1965

REFERENCES

1. Croom, Delwin; Naeseth, Rodger L.; and Sleeman, William C., Jr.: Low Speed Wind-Tunnel Investigation of Effects of Canopy Shape on the Aerodynamic Characteristics of a 55° Swept Parawing Having a Large Diameter Leading Edges. NASA TN D-2551, 1964.

2. Sleeman, William C., Jr.: Low-Speed Investigation of Cable Tension and Aerodynamic Characteristics of a Parawing and Spacecraft Combination. NASA TN D-1937, 1963.

3. Naeseth, Rodger L.; and Gainer, Thomas G.: Low-Speed Investigation of the Effects of Wing Sweep on the Aerodynamic Characteristics of Parawings Having Equal-Length Leading Edges and Keel. NASA TN D-1957, 1963.

TABLE I.- MODEL DIMENSIONS AND MATERIALS

Area	
Flat pattern	569.4 ft^2
Deployed, reference, S	536.2 ft^2
Span	1.15 l_k
Boom length, l_k, reference	366.9 in.
Boom diameter	0.060 l_k
Spreader bar diameter	0.044 l_k
Leading-edge sweep	
Sail flat pattern	52.5°
Boom	55.0°
Suspension line diameter	0.25 in.
Nylon bungee length	
l_f	46.6 in.
l_d	34.3 in.
l_a	28.8 in.
l_c	38.8 in.
Materials	
Sail and load distribution curtain	polyester fabric
Inflatable structure	neoprene coated Dacron fabric
Load distributor cable and boltrope	nylon
Suspension lines	steel

A-31565

Figure 1.- Paraglider model mounted in the Ames 40- by 80-Foot Wind Tunnel.

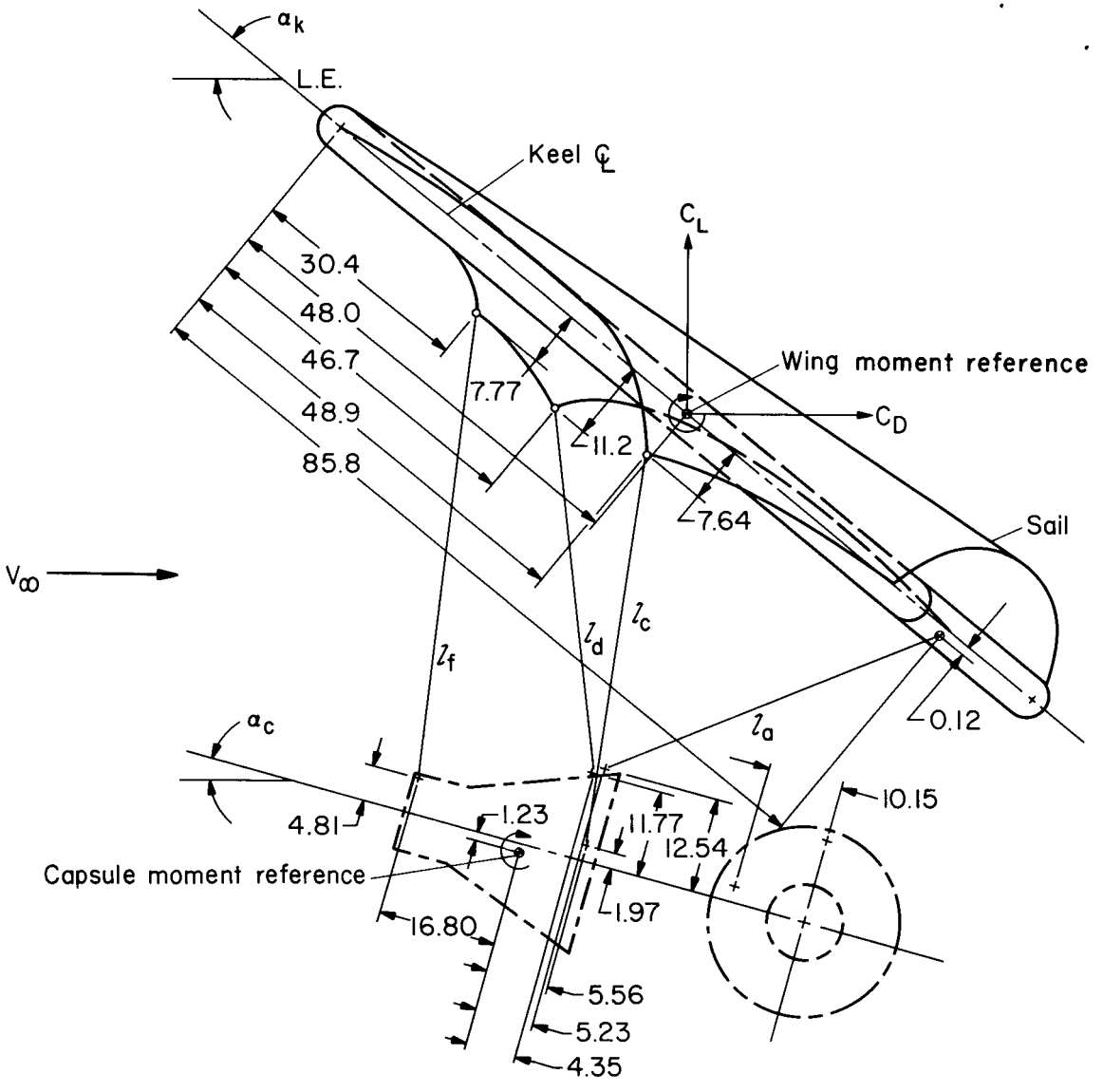

(a) Suspension line attachment points.

Figure 2.- Model dimensions and arrangement.

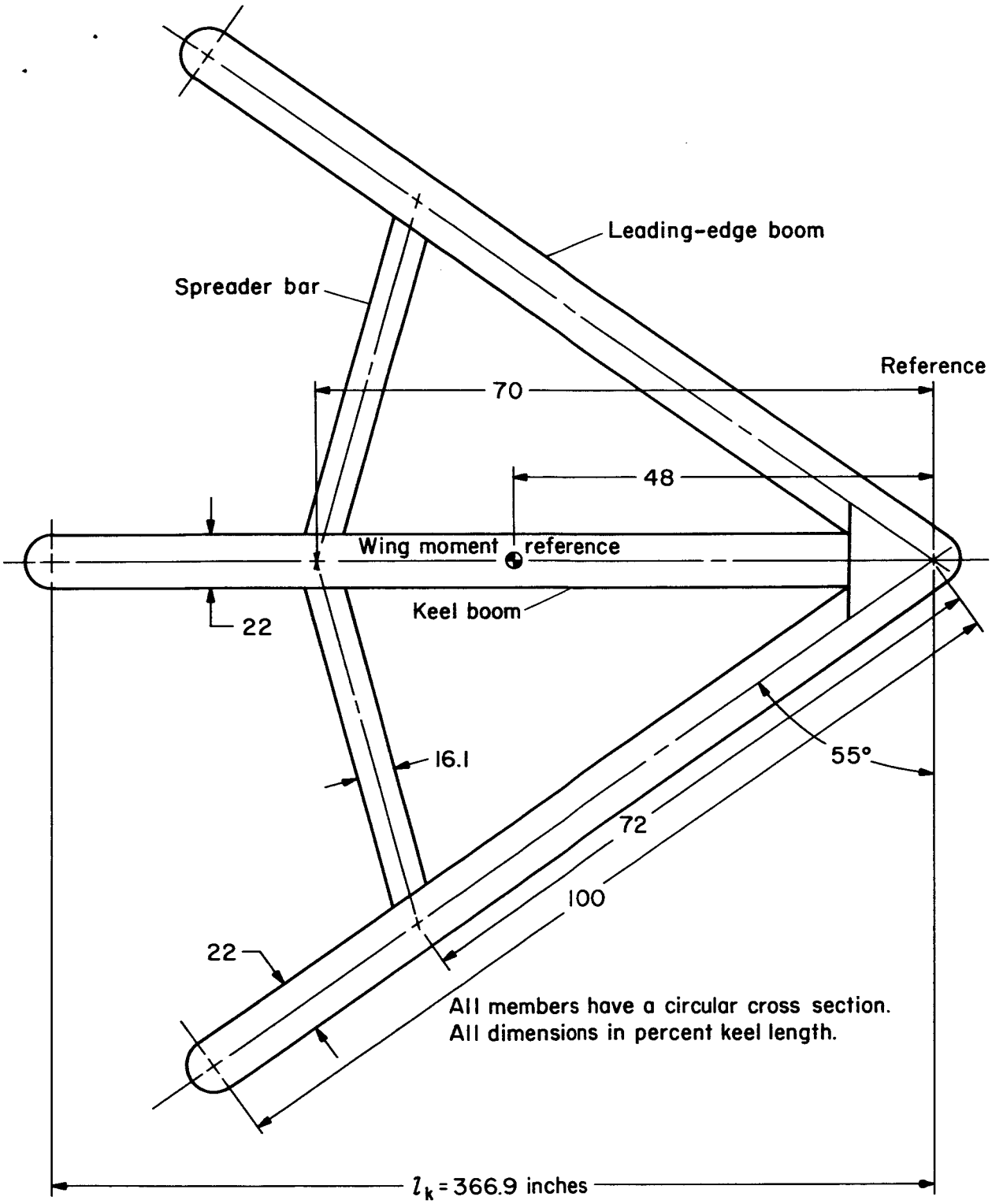

(b) Inflatable structure.

Figure 2.- Concluded.

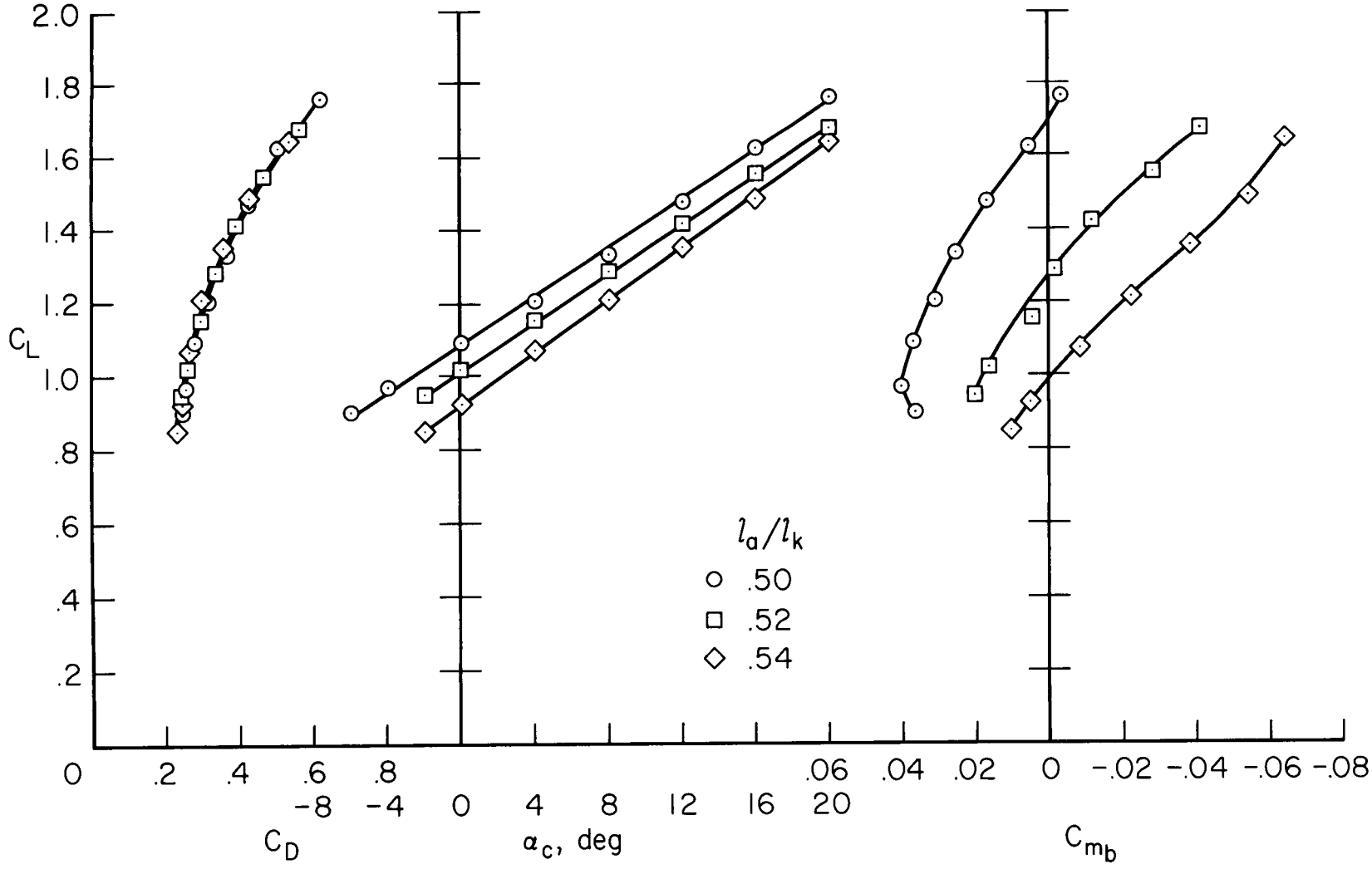

(a) l_f/l_k = 0.61

Figure 3.- Aerodynamic characteristics for several combinations of suspension line lengths with the metal spreader bar sleeves; q = 7-1/2 psf.

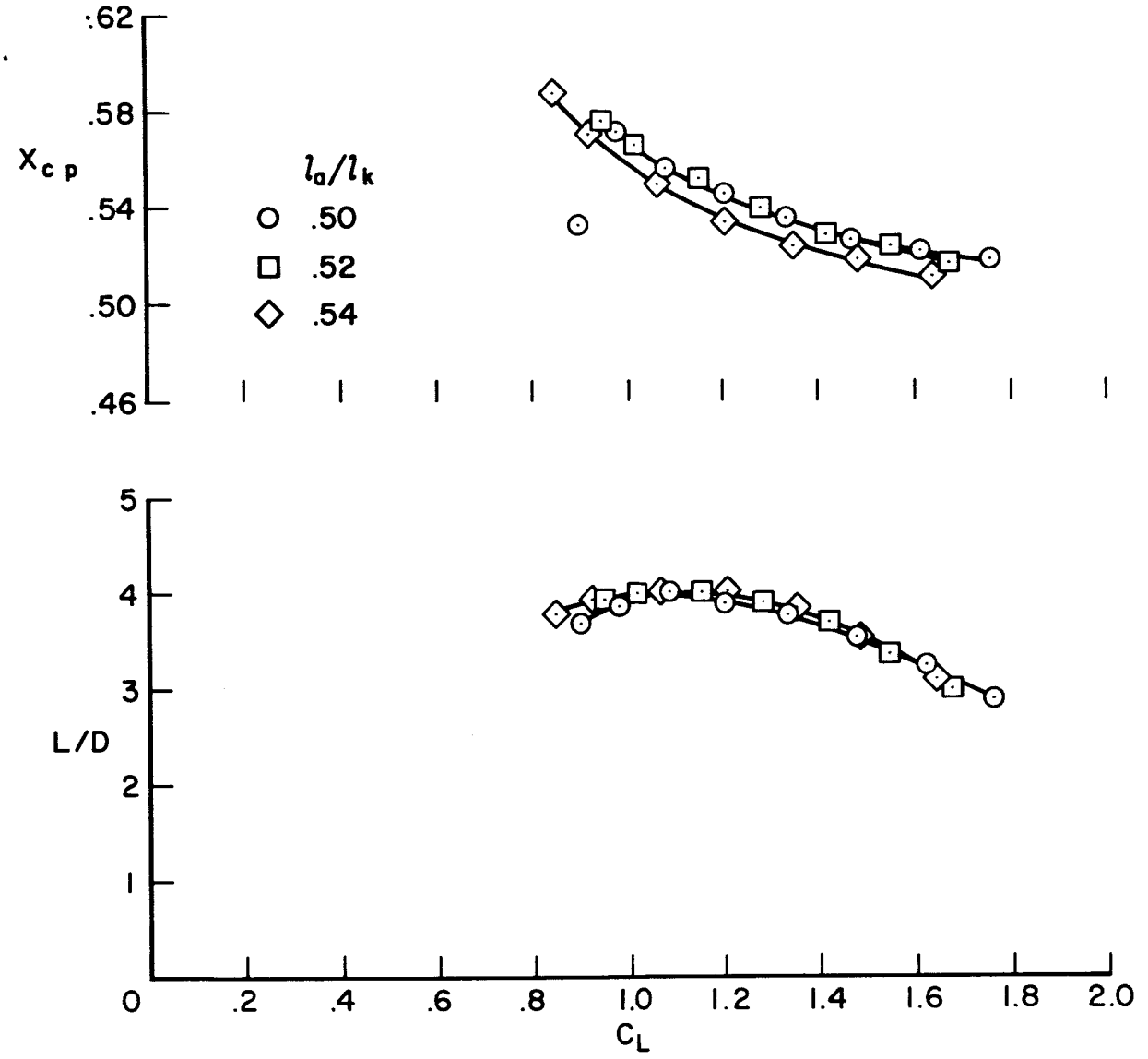

(a) l_f/l_k = 0.61 - Concluded

Figure 3.- Continued.

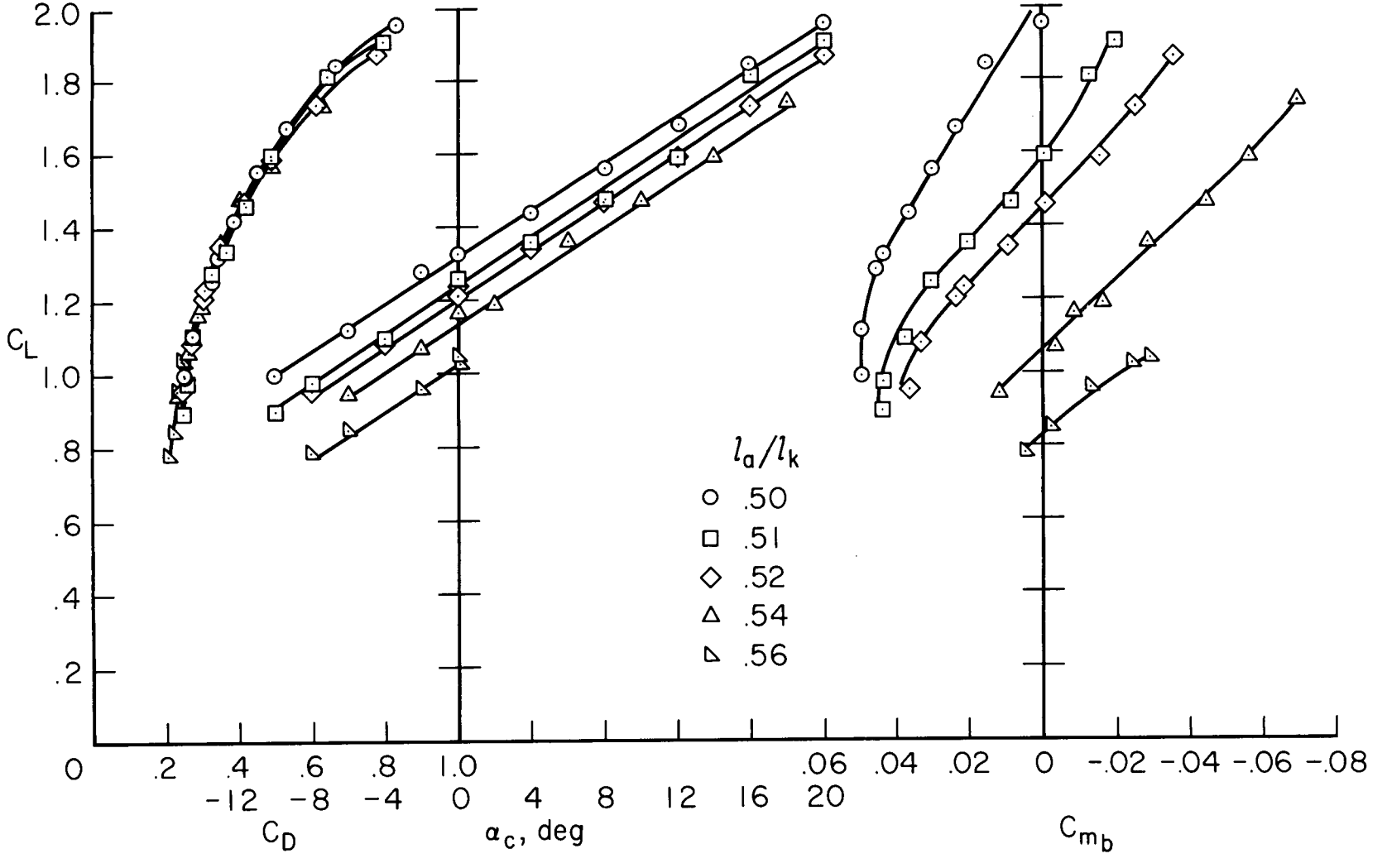

(b) l_f/l_k = 0.63

Figure 3.- Continued.

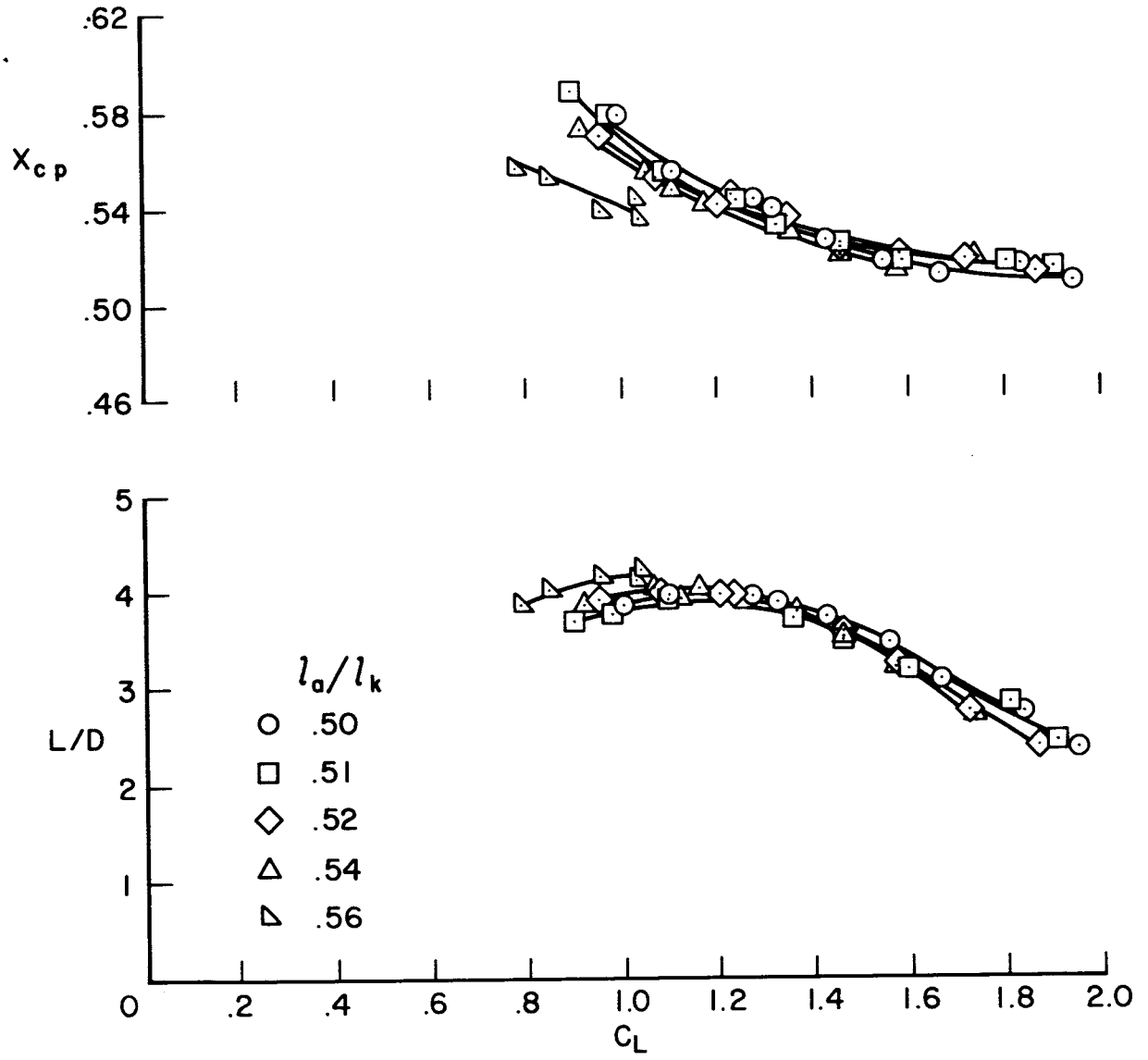

(b) l_f/l_k = 0.63 - Concluded

Figure 3.- Continued.

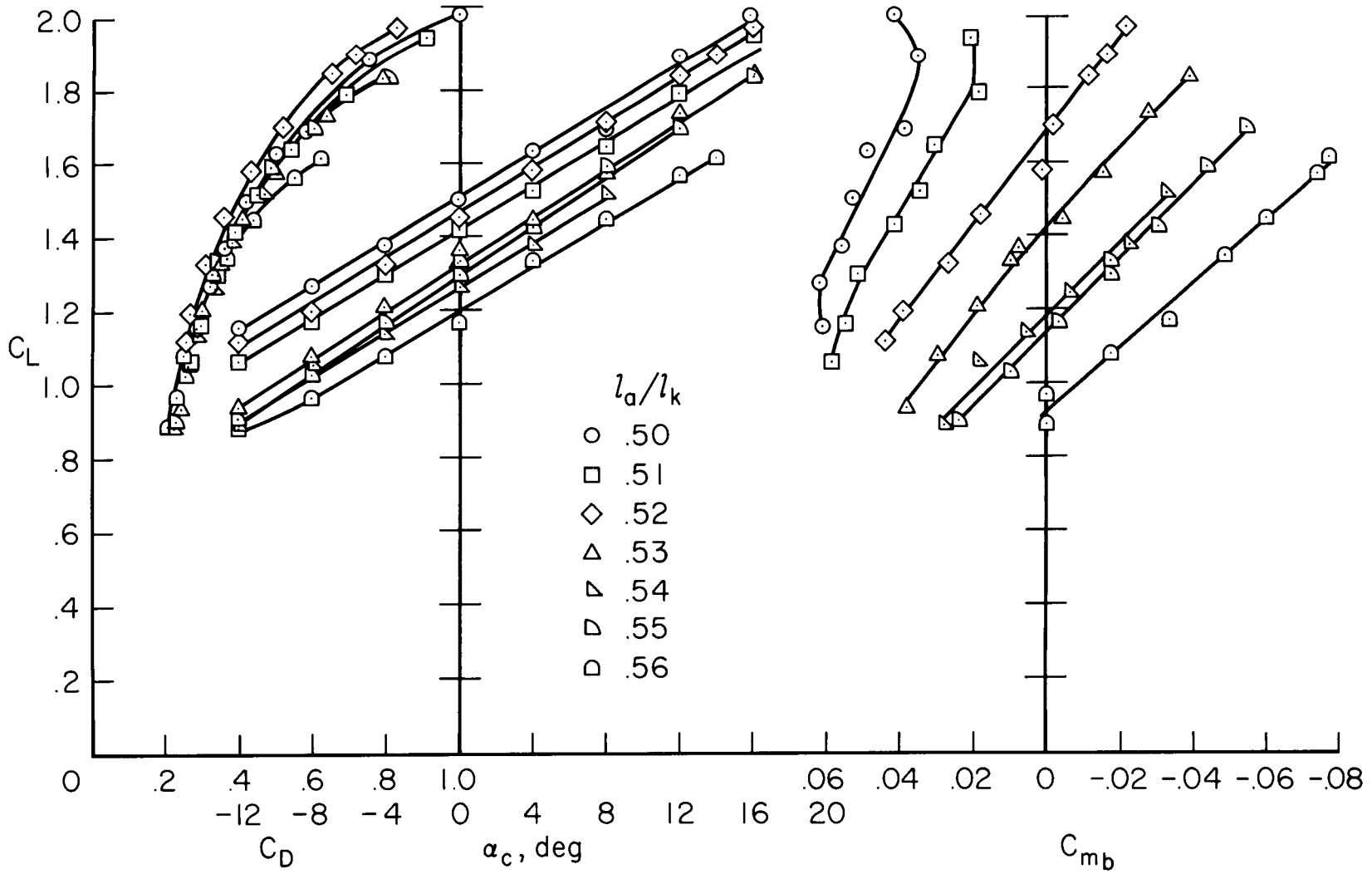

(c) l_f/l_k = 0.65

Figure 3.- Continued.

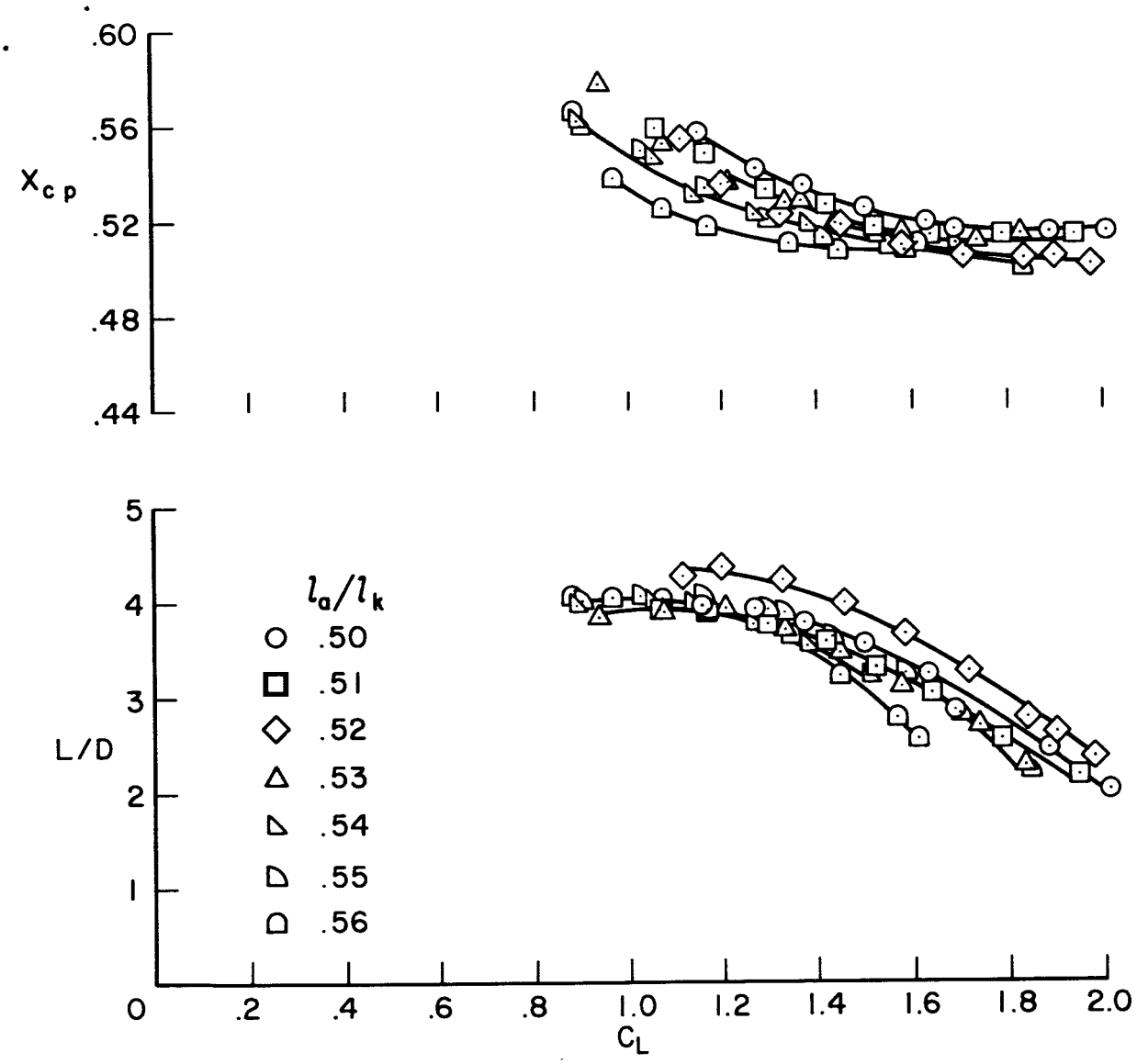

(c) l_f/l_k = 0.65 - Concluded

Figure 3.- Continued.

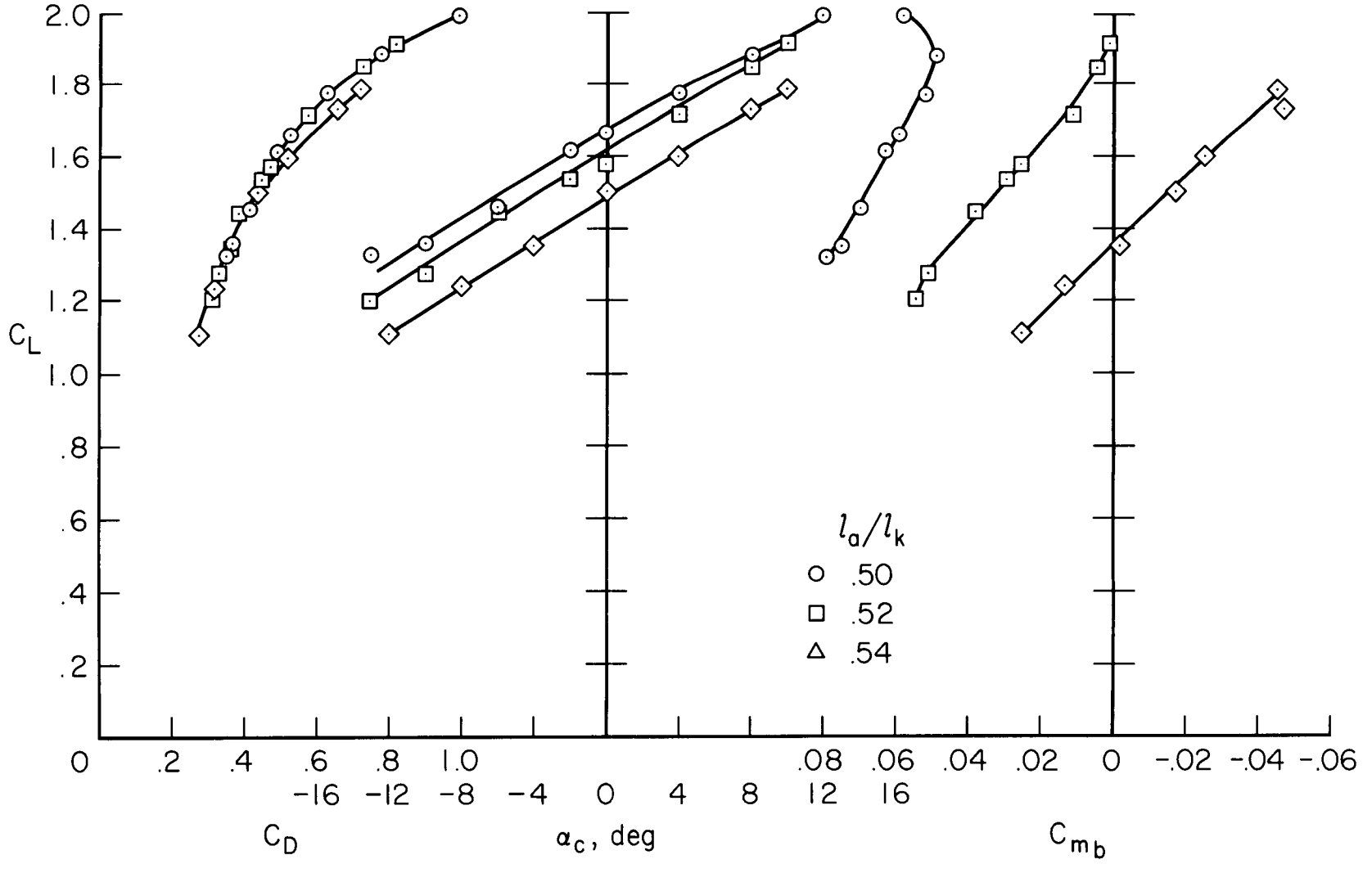

(d) l_f/l_k = 0.67

Figure 3.- Continued.

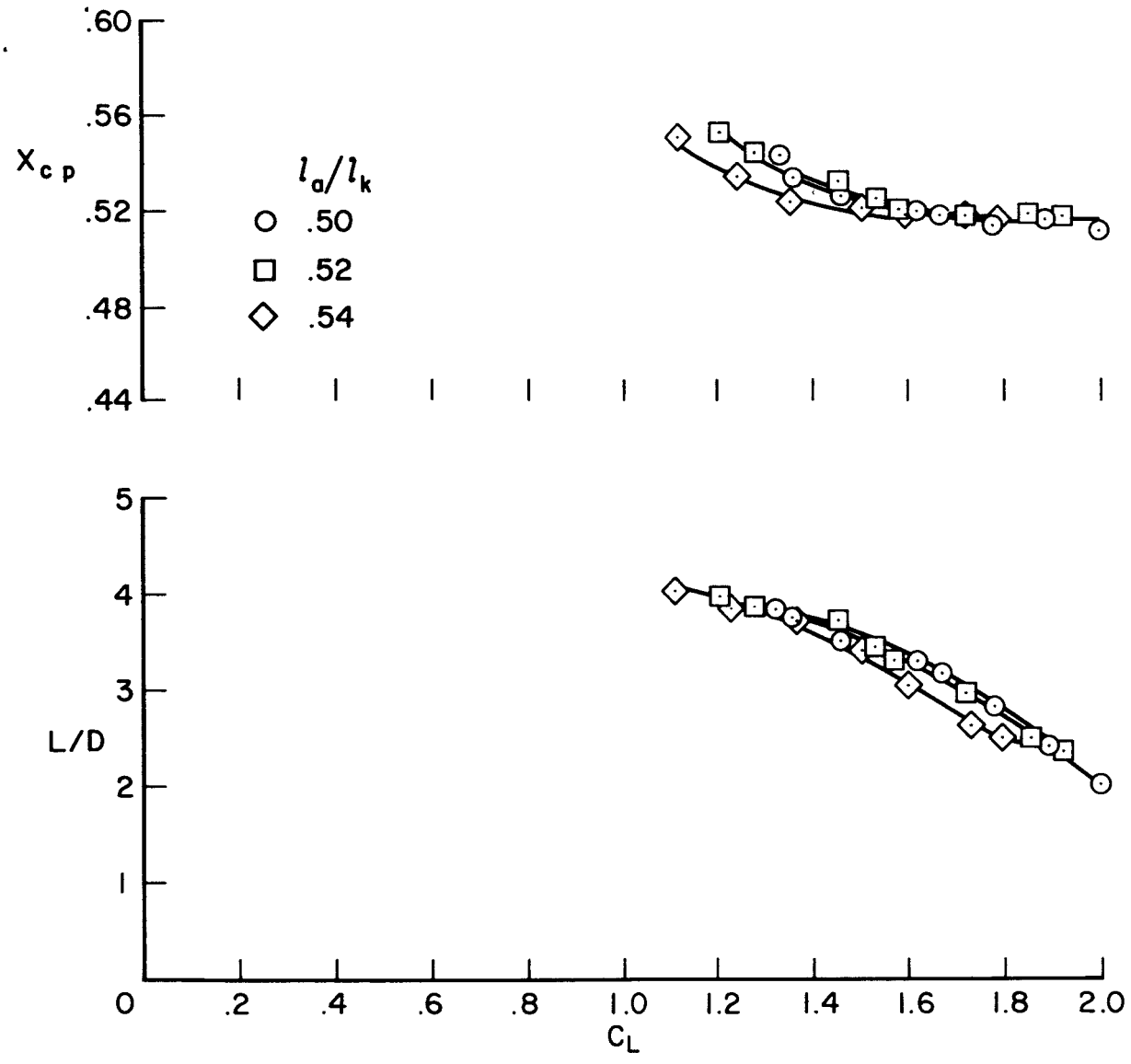

(d) l_f/l_k = 0.67 - Concluded

Figure 3.- Concluded.

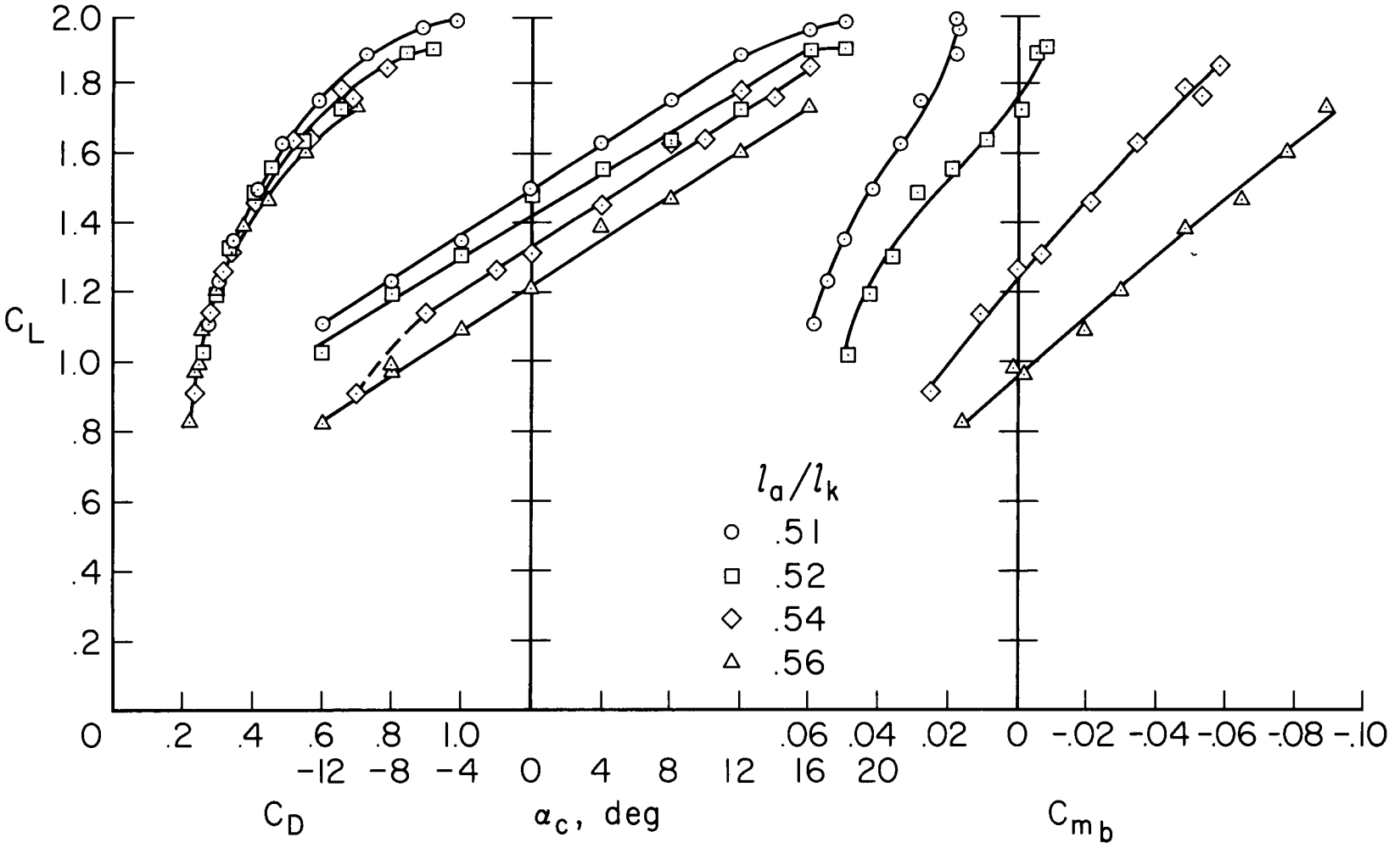

(a) C_L as a function of C_D, α_c, and C_{m_b}.

Figure 4.- Aerodynamic characteristics for several combinations of suspension line lengths with the fabric spreader bar sleeves; q = 7-1/2 psf, l_f/l_k = 0.65.

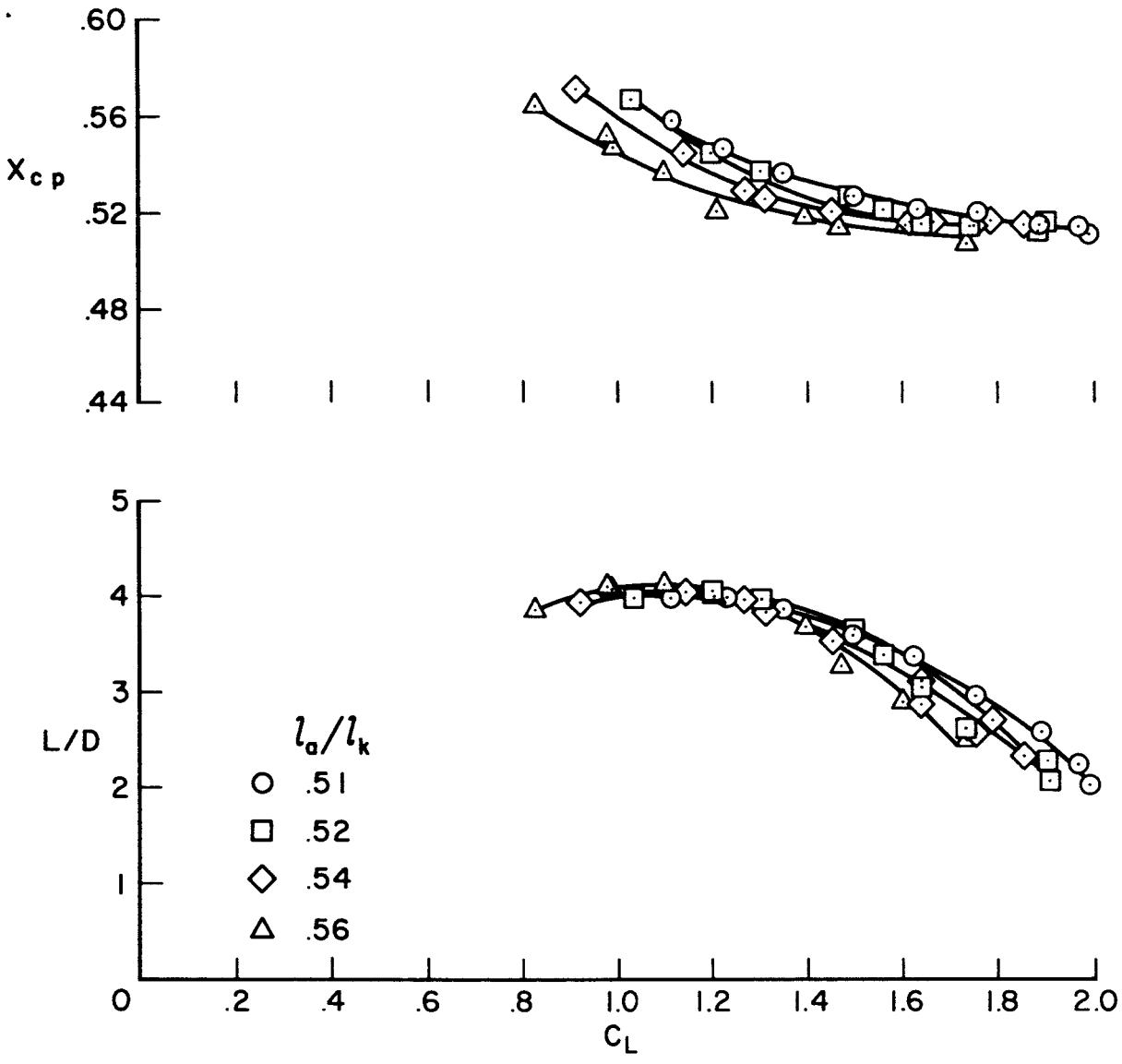

(b) Center of pressure and L/D as functions of C_L.

Figure 4.- Concluded.

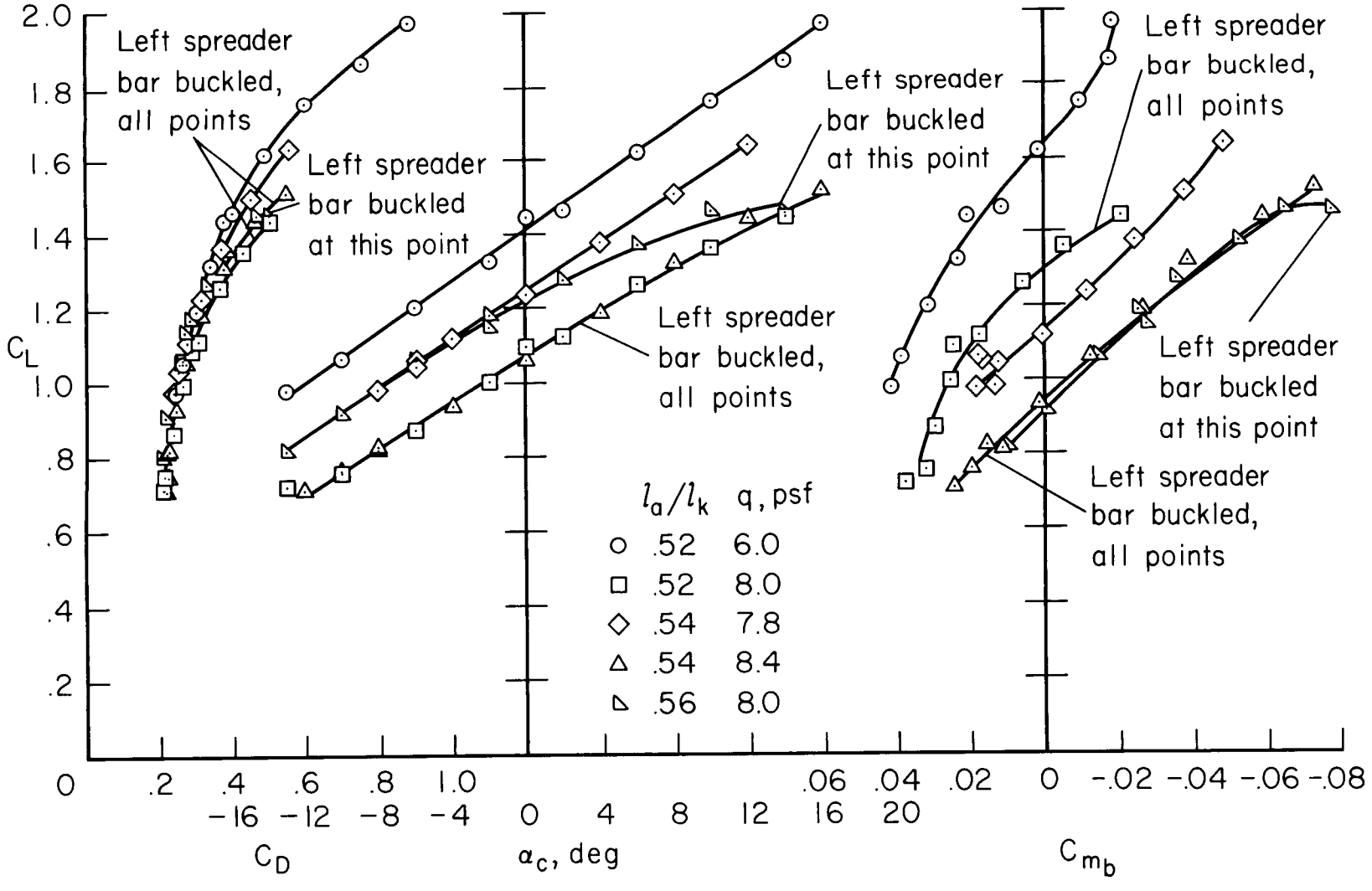

(a) C_L as a function of C_D, α_c, and C_{m_b}.

Figure 5.- Aerodynamic characteristics for several combinations of suspension line lengths with the basic spreader bars; $l_f/l_k = 0.65$.

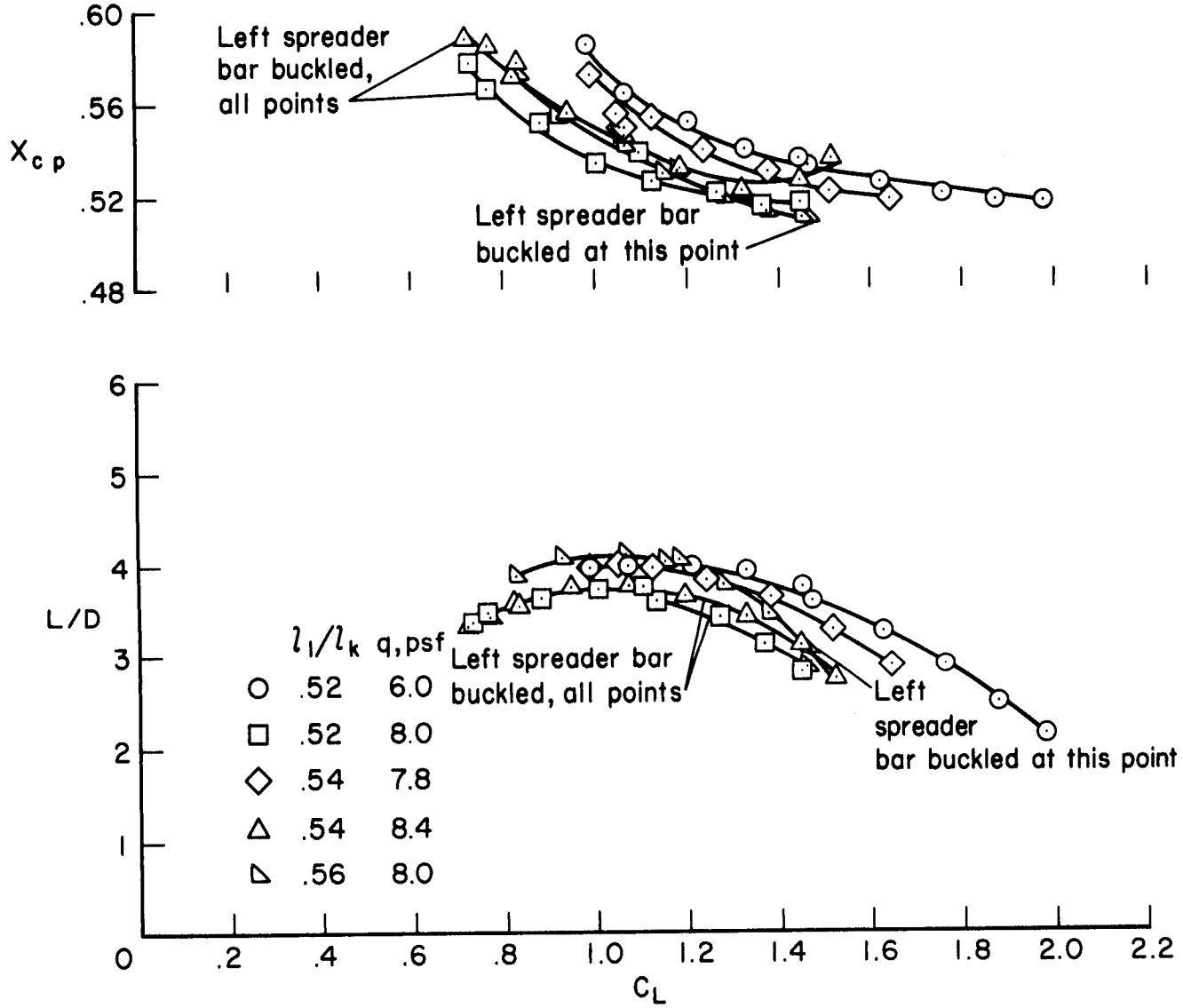

(b) Center of pressure and L/D as functions of C_L.

Figure 5.- Concluded.

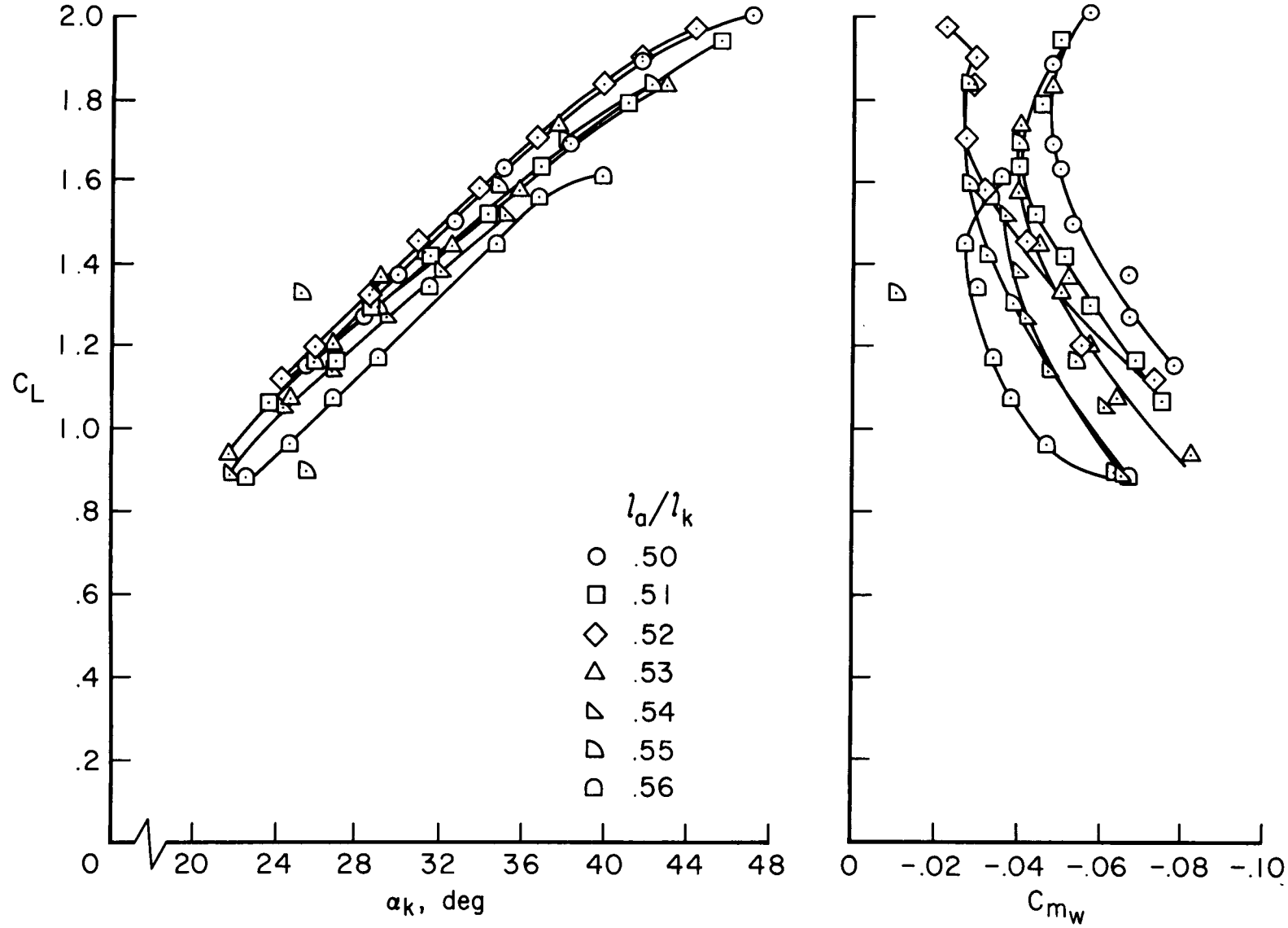

Figure 6.- Aerodynamic characteristics referred to wing angle of attack and moment reference; l_f/l_k = 0.65, q = 7-1/2 psf, metal spreader bar sleeve.

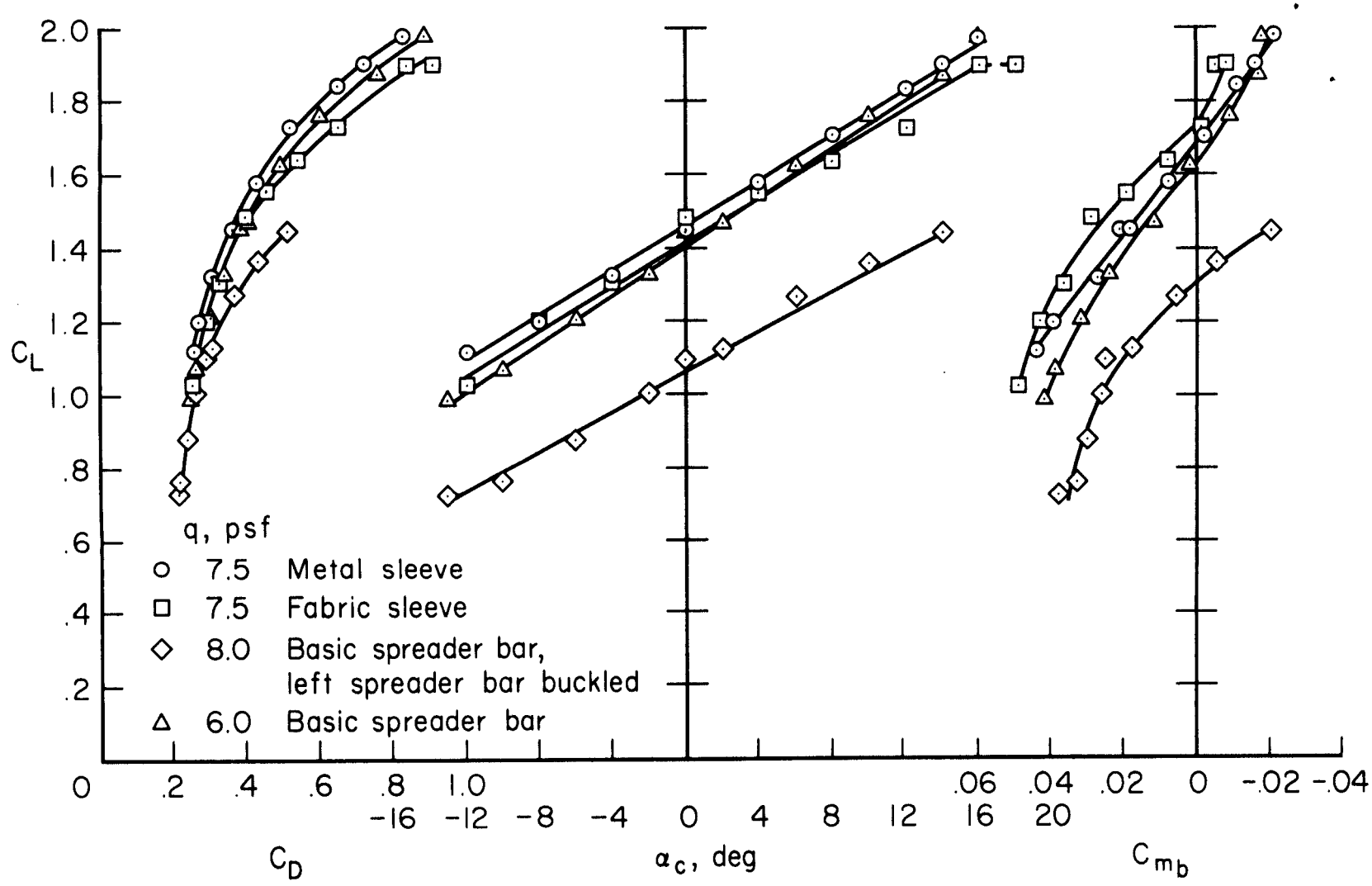

(a) C_L as a function of C_D, α_c, and C_{m_b}.

Figure 7.- Comparison of the aerodynamic characteristics for the three spreader bar configurations; $l_f/l_k = 0.65$, $l_a/l_k = 0.52$.

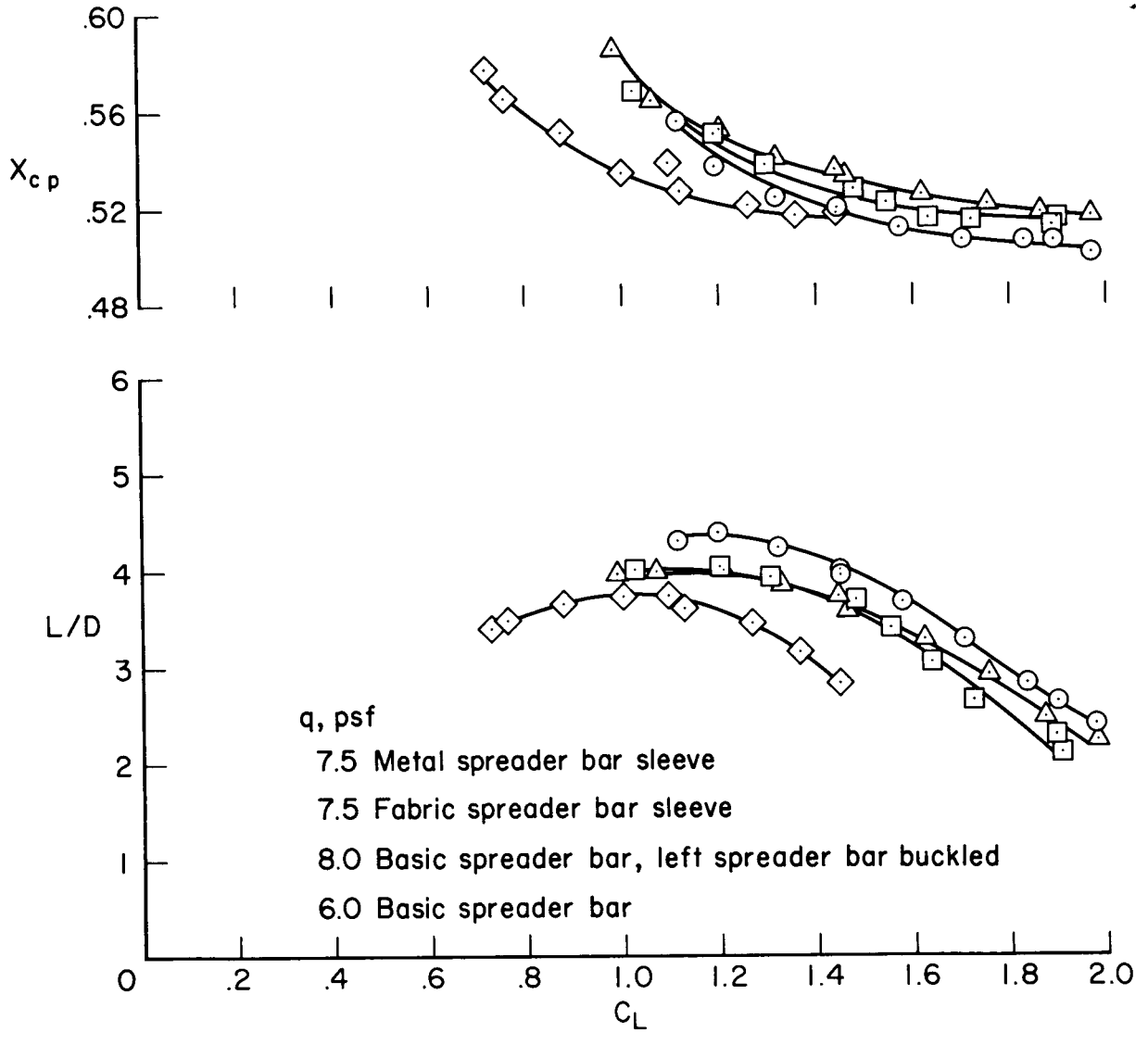

(b) Center of pressure and L/D as functions of C_L.

Figure 7.- Concluded.

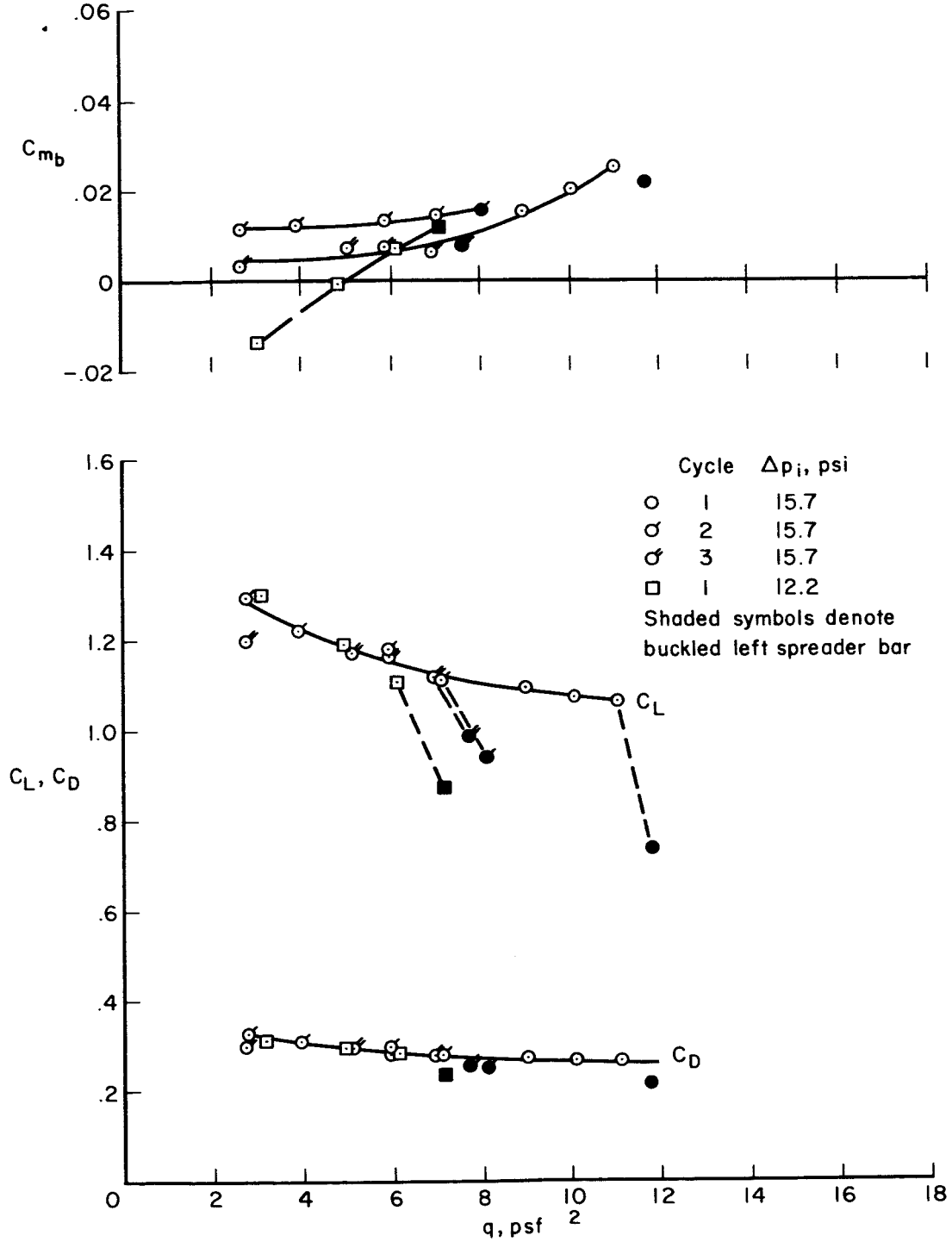

(a) Basic spreader bars.

Figure 8.- Effect of dynamic pressure on aerodynamic characteristics with and without the fabric spreader bar sleeve; $l_f/l_k = 0.65$, $l_a/l_k = 0.54$, $\alpha_c = -6^\circ$.

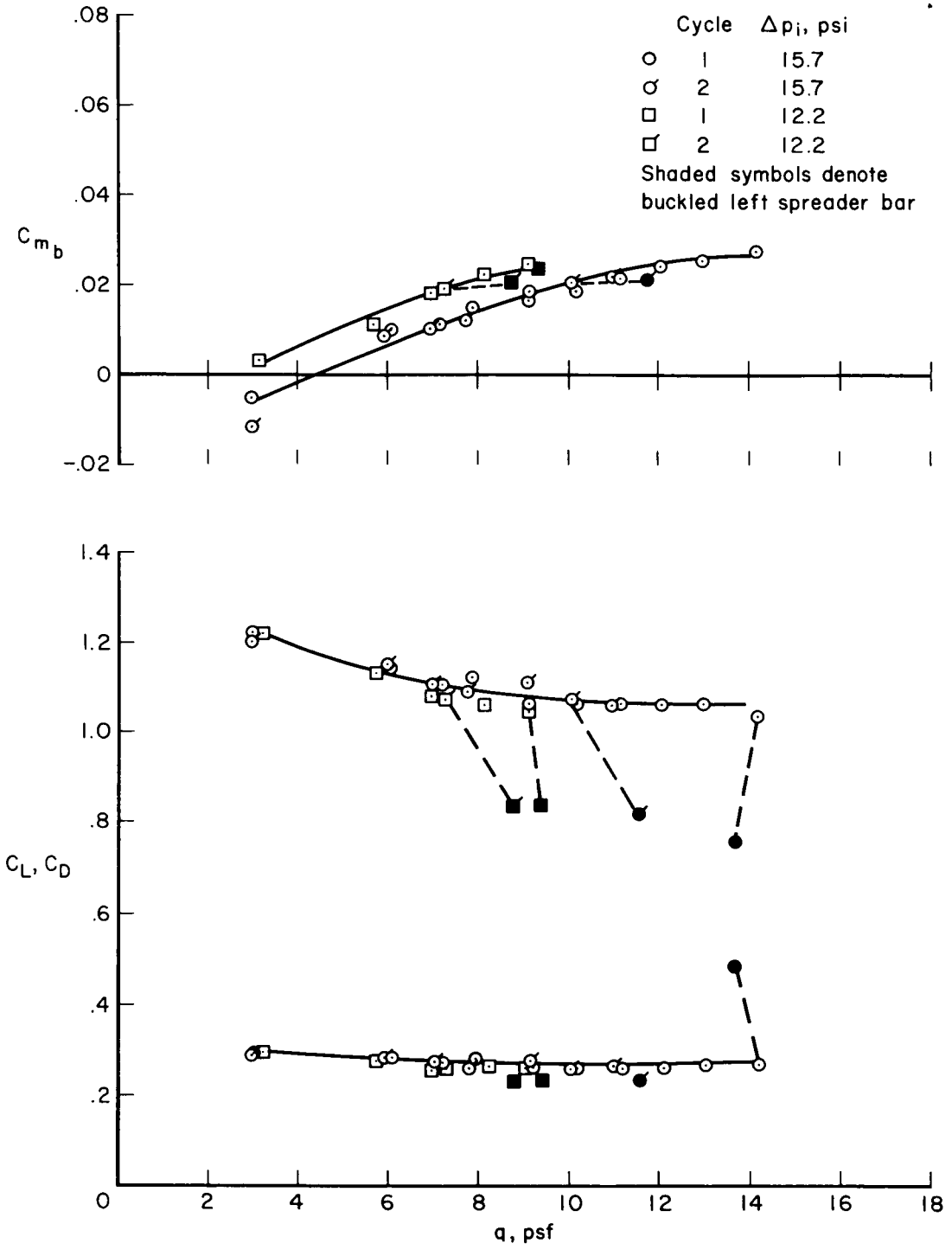

(b) Fabric spreader bar sleeves.

Figure 8.- Concluded.

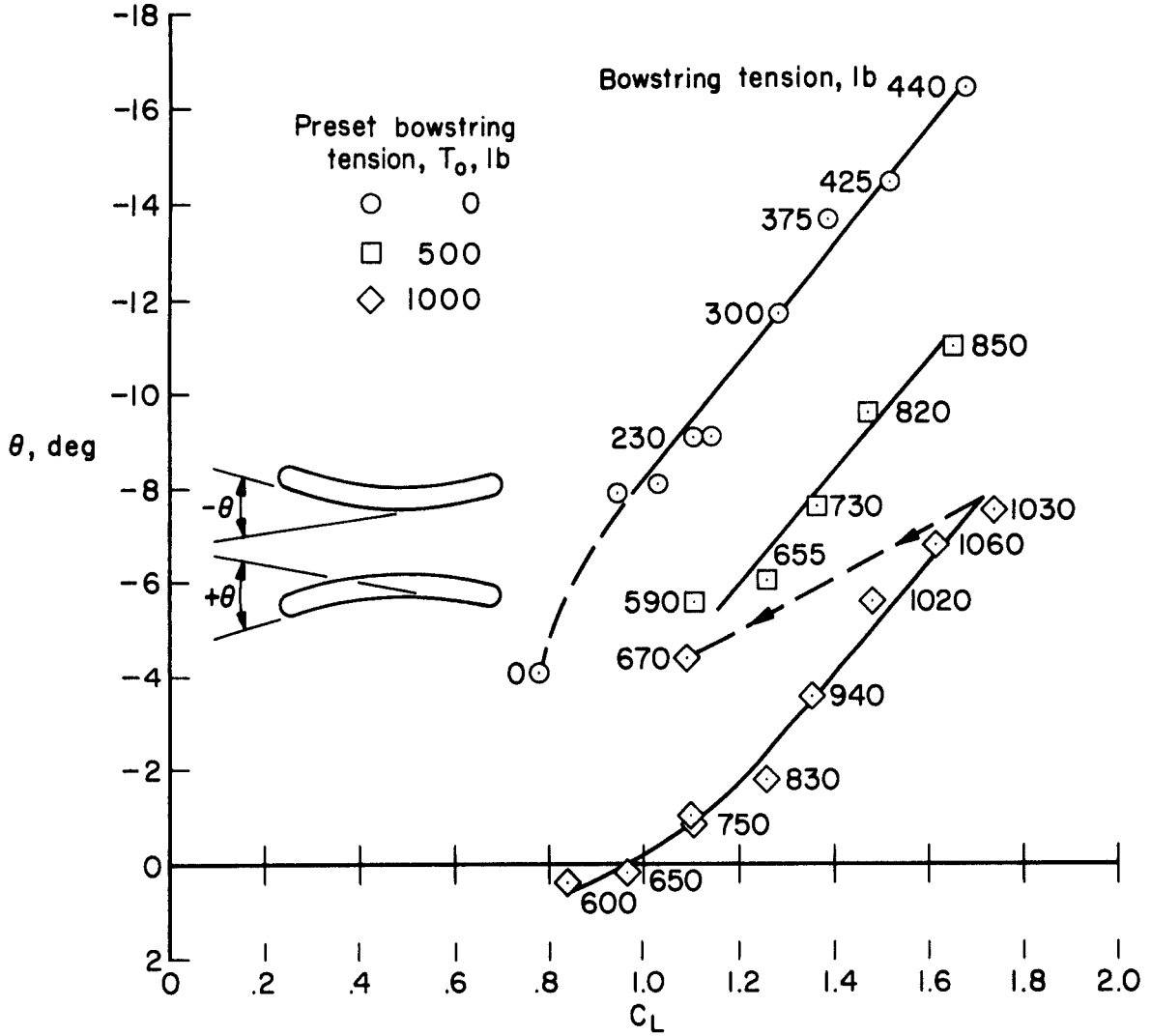

(a) Variation of keel comber and bowstring tension with C_L.

Figure 9.- Keel boom deformation for three preset tensions; basic spreader bars, l_f/l_k = 0.63, l_a/l_k = 0.54, q = 7-1/2 psf.

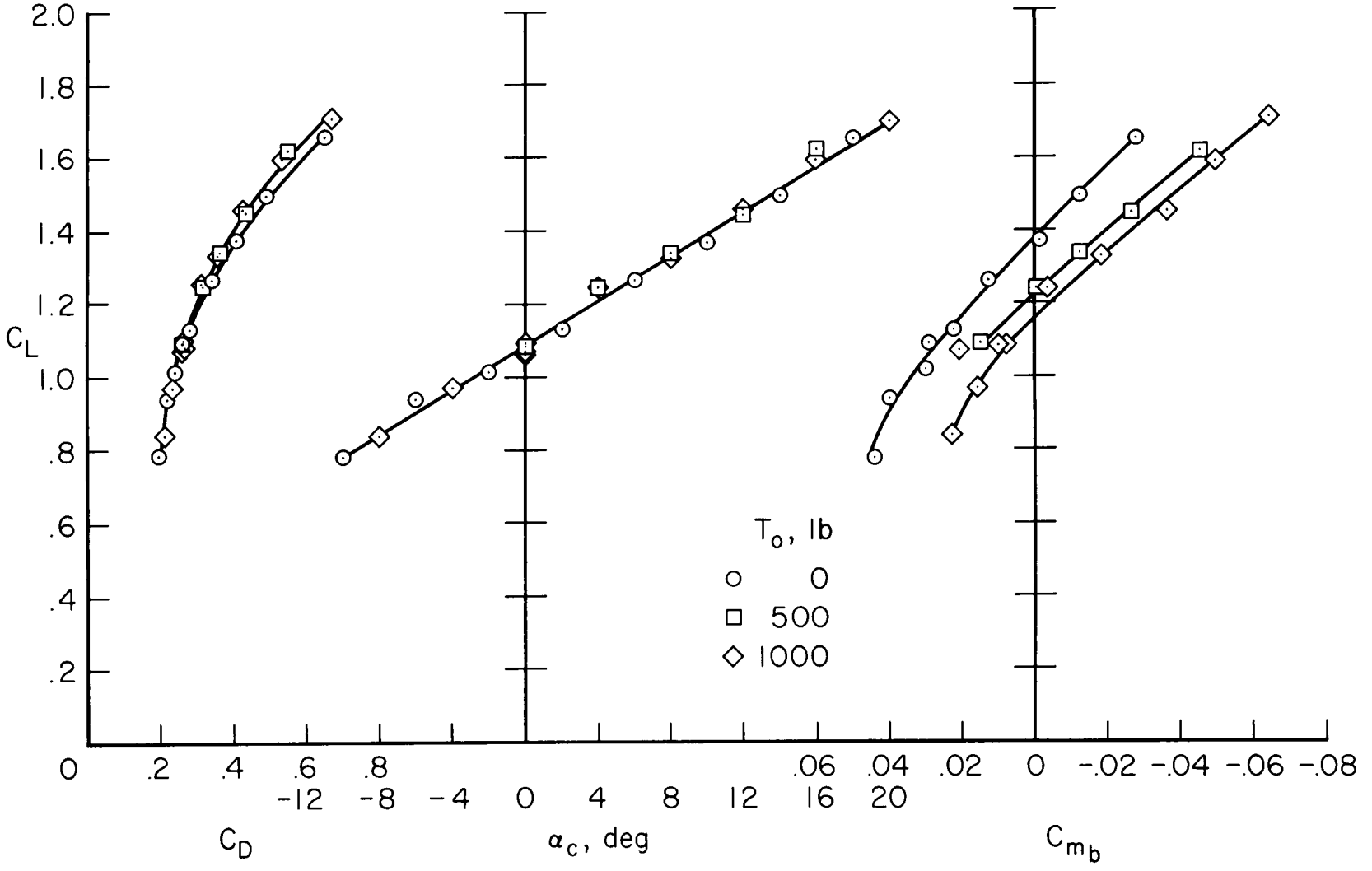

(b) Effect on aerodynamic characteristics.

Figure 9.- Concluded.